

HARMONIC ANALYSIS OF A FIVE LEVEL CASCADED INVERTER UNDER A NEW MODULATION SCHEME

AZIZ, J.¹ & SALAM, Z.²

Abstract. This paper proposes an analytical method to predict the incidence and magnitude of harmonics of the output voltage of a five-level cascaded inverter. The cascaded inverter is subjected to a new modulation scheme, which uses multiple modulating signals with a single carrier. From the modulation scheme, mathematical equations that define the PWM switching instants are derived. In order to justify the merits of the proposed modulation scheme, harmonic analysis for the Fourier coefficients is outlined and calculated using MATLAB. An experimental five-level cascaded inverter test-rig is built and the new modulation scheme is implemented. The calculated and measured harmonics of the output voltage are compared and discussed.

Key words: Harmonic analysis, cascaded inverter

Abstract. Kertas kerja ini mengusulkan satu kaedah analitikal untuk meramalkan magnitud dan kedudukan harmonik voltan keluaran penyongsang lima tahap. Penyongsang tersebut telah digunakan untuk melaksanakan satu skim pemodulatan baru yang menggunakan beberapa isyarat memodulat berserta isyarat pembawa tunggal. Seterusnya daripada skim pemodulatan tersebut, persamaan matematik yang dapat menentukan pensuisan PWM diterbitkan. Untuk memastikan kelebihan skim pemodulatan tersebut, analisis harmonik untuk mendapatkan pekali Fourier diterbitkan dan dikira menggunakan MATLAB. Harmonik voltan keluaran yang diukur dan dikira seterusnya dibandingkan dan dibincangkan.

Kata kunci: Analisis harmonik, penyongsang bertahap

1.0 INTRODUCTION

Multilevel inverter has become an effective and practical solution for reducing switching losses in high power voltage source inverter (VSI) applications [1,2]. By synthesizing the ac output voltage from several levels of dc voltages, a staircase or multilevel output waveform is produced. For a conventional VSI, the maximum voltage level output is determined by the voltage blocking capability of each device. In many cases, the power device blocking capability could not reach the required DC link voltage, hence limiting their application. Ingenious methods, such as device series connection to increase the blocking capacity may result in very complicated and unreliable circuits [2]. By using a multilevel structure, the stress on each device can be reduced in

^{1&2} Faculty of Electrical Engineering, Universiti Teknologi Malaysia, UTM 81310 Skudai, Johor Bahru, Johor. Malaysia. Tel: +607-553 5363. Fax: +607-556 6272. Contact e-mail: zainals@suria.fke.utm.my

proportional to the number of levels, thus the inverter can handle higher voltages [3]. It may be possible, in certain application to avoid expensive and bulky step-up transformers.

Another significant advantage of a multilevel output waveform is that several voltage levels leads to a better and more sinusoidal voltage waveform. As a result, a lower total harmonic distortion (THD) is obtained. In another perspective, the harmonic in the output waveform can be reduced without increasing switching frequency or decreasing the inverter power output [4]. As the number of voltage levels reach infinity, the output THD approaches zero. The number of the achievable voltage levels, however, is limited by voltage unbalance problems, voltage clamping requirement, circuit layout, and packaging constraints.

In motor application, high dV/dt in power supply generates high stress on motor windings and requires additional motor insulation. Furthermore, high dV/dt of semiconductor devices increases the electromagnetic interference (EMI), common-mode voltage and possibility of failure on motor. With several levels in output waveform constructed by multilevel inverter, the switching dV/dt stresses are reduced [3].

With these known advantages, multilevel VSI has become a popular alternative to the conventional VSI. There are various works carried out in this area but there appear to be limited publications on the analytical method to calculate the harmonics spectra of the output voltage. This paper is meant to bridge this gap.

In this work an analytical method to predict the incidence and the magnitude of harmonics of the output voltage of a five-level cascaded inverter is presented. A five-level cascaded inverter topology circuit and the new modulation scheme is implemented. The calculated and experimental result is compared.

2.0 CASCADED INVERTER

There are three main types of multilevel inverter topologies that are frequently cited in literature: (1) diode-clamped multilevel inverters (DCMI), (2) flying capacitor multilevel inverters (FCMI) and (3) cascaded inverters. Abovementioned topologies have their specific advantages and disadvantages as detailed elsewhere [1,2]. The last topology (cascaded inverter) uses cascaded inverters with separate dc sources, and hence it is naturally well suited for various renewable energy sources such as photovoltaic, fuel cell and biomass. The cascaded inverter requires the least number of components among all multilevel converters to achieve the same voltage levels. It also avoids the necessity for complicated clamping diodes or voltage balancing capacitors. Moreover modularized circuit layout and packaging is possible because each voltage level is synthesized using a regular inverter structure.

A single-phase N-level cascaded inverter configuration is shown in Figure 1. It consist a several single-phase full-bridge (H-bridge) inverter modules with separate dc sources. The ac output voltage of each module is connected in series to form an output voltage, V_o . The number of module (M), which is equal to the number of dc sources, depends

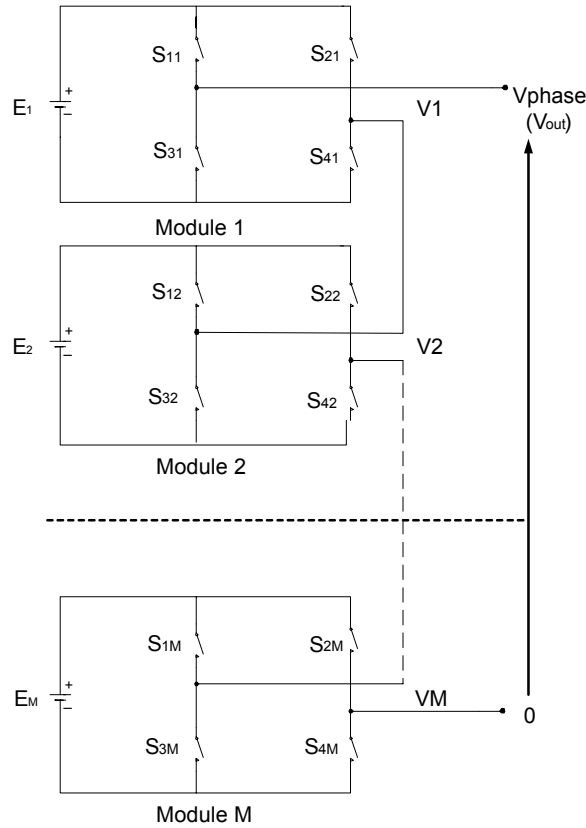


Figure 1 Single-phase structure of a cascaded inverter

on the number of levels (N) required. It is usually assumed that N is odd, as this would give an integer-valued M . The number of output voltage levels is defined by:

$$M = \frac{N - 1}{2} \quad (1)$$

By different combinations of the four switches, S_{1M} through S_{4M} , each module can generate three different voltage outputs, i.e. $+E$, $-E$, and 0 . The total output voltage is constructed by the sum of the output voltage from each module. For example, a five level inverter would have an output levels of $+2E$, $+E$, 0 , $-E$, and $-2E$.

3.0 THE PROPOSED MODULATION SCHEME [5]

The proposed modulation scheme for the cascaded inverter is based on the classical unipolar, symmetric PWM switching technique. The main idea behind this method is to compare several modified sinusoidal modulation signals $s(k)$ with a single triangular carrier signal $c(k)$ as shown in Figures 2 and 3. These modified signals are the “regular

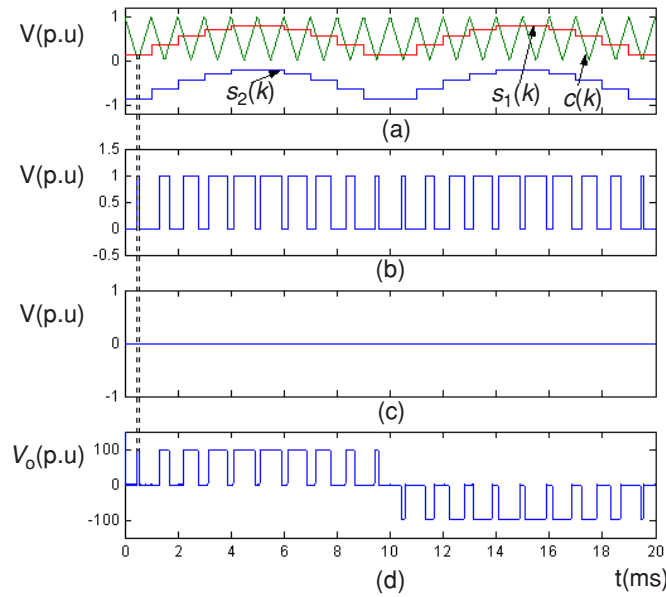


Figure 2 Principal of the proposed modulation scheme for $m_i = 0.4$, $m_f = 20$

(a) Modulation signals and carrier signal; (b) PWM pulses produced from comparison between $s_1(k)$ and $c(k)$, $V_1(k)$; (c) PWM pulses produced from comparison between $s_2(k)$ and $c(k)$, $V_2(k)$; (d) PWM output waveform, $V_o(V)$.

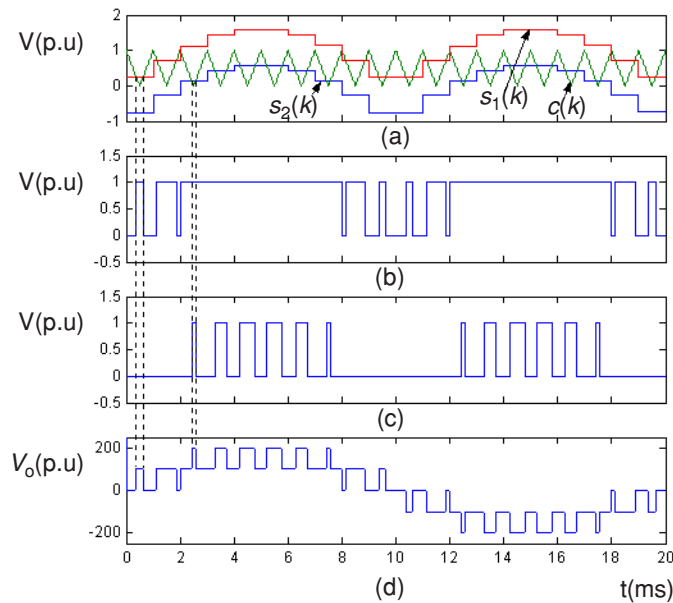


Figure 3 Principal of the proposed modulation scheme for $m_i = 0.8$, $m_f = 20$.

(a) Modulation signals and carrier signal; (b) PWM pulses produced from comparison between $s_1(k)$ and $c(k)$, $V_1(k)$; (c) PWM pulses produced from comparison between $s_2(k)$ and $c(k)$, $V_2(k)$; (d) PWM output waveform, $V_o(V)$.

sampled” of the continuous sinusoidal modulating waveforms, $m(t)$. Intersection between the modified modulation signals and the carrier signal defines the switching instant of the PWM pulses. Each of these modified modulation signals have the same frequency (f_o) and amplitude (A_m). Since the modulation is symmetric, the modulation signals are sampled once in every carrier cycle. The output waveform obtained is quarter wave symmetry. The carrier signal is a train of triangular waveform with frequency f_c and amplitude A_c .

Equations (2) defines the modulation index m_i for N-level inverter with M number of modules:

$$m_i = \frac{A_m}{\frac{(N-1)}{2} A_c} = \frac{A_m}{M A_c} \quad (2)$$

Therefore if A_c defined at a fixed p.u (1p.u), then m_i ranges between 0 and 1, while A_m ranges between 0 and M. The definition of the modulation ratio m_f for multilevel inverter is similar to the conventional two-level output inverter, i.e.:

$$m_i = \frac{f_c}{f_o} \quad (3)$$

In this Equation, f_c and f_o correspond to the frequencies of the carrier and sinusoidal modulation signals, respectively. To illustrate the principal of the proposed scheme, a five-level inverter at $m_i = 0.4$ and $m_i = 0.8$ is shown in Figure 2 and 3, respectively. For clarity, m_f for both cases was arbitrary chosen to be a low value of 20. For a five level output, two modulation signals namely $s_1(k)$ and $s_2(k)$ and single triangular carrier $c(k)$ are involved in the modulation process. Signal $s_2(k)$ actually is $s_1(k)$ that shifted down by the amplitude of triangular carrier signals A_c .

The PWM pulses $V_1(k)$ is generated from the comparison between $s_1(k)$ and $c(k)$, while $V_2(k)$ is from comparison between $s_2(k)$ and $c(k)$. The comparison is designed such that if $s_1(k)$ is greater than $c(k)$, a pulse-width $V_1(k)$ is generated; if $s_2(k)$ is greater than $c(k)$, $V_2(k)$ is generated. On the other hand if there is no intersection, then $V_1(k)$ and $V_2(k)$ remain at 0. It can be seen in Figure 2 that for the case of $m_i \leq 0.5$, only $s_1(k)$ and carrier signal $c(k)$ is involved in the modulation process. There is no intersection for $s_2(k)$. Therefore, the output pulse $V_1(k)$ is zero. The output voltage $V_o(k)$, which is the sum of $V_1(k)$ and $V_2(k)$, is then similar to the conventional three-level unipolar PWM case. For $m_i > 0.5$, as depicted in Figure 3, both modulating signal, i.e. $s_1(k)$ and $s_2(k)$ intersect the carrier and therefore $V_1(k)$ and $V_2(k)$ pulses are generated. As a result, a five-level output voltage $V_o(k)$ is formed.

Previous works [5] has shown that a simple algorithm, expressed by Equation (4), could be used to calculate the switching instants for the proposed modulation scheme. The equations can be easily implemented in hardware using digital technique.

$$\alpha_U(k) = \frac{T_c}{2} \left[(2k - U - 2) - \frac{A_m}{A_c} \sin \left(\omega(k-1) + \frac{\pi}{m_f} \right) \right] \quad (4)$$

where $k = 1, 2, \dots, \frac{m_f}{2}$ and $U = 1, 2, \dots, M$.

For example, for a five-level cascaded inverter which has 2 modules ($M = 2$). Equation (4) can be expressed as:

$$\alpha_1(k) = \frac{T_c}{2} \left[(2k - 1) - \frac{A_m}{A_c} \sin \left(\omega(k-1) + \frac{\pi}{m_f} \right) \right] \quad (4.1)$$

$$\alpha_2(k) = \frac{T_c}{2} \left[2k - \frac{A_m}{A_c} \sin \left(\omega(k-1) + \frac{\pi}{m_f} \right) \right] \quad (4.2)$$

4.0 DERIVATION OF HARMONIC COEFFICIENTS

This section presents an analytical method to obtain the Fourier coefficients for a five-level cascaded inverter using the proposed modulation scheme. The purpose is to predict the magnitude and incidence of the harmonics of the output voltage. As noted earlier, for the case of $m_i \leq 0.5$, a three-level output voltage is produced. In this situation, the derivation of Fourier coefficient is similar to the normal regular sampled sinusoidal PWM. However, for $m_i \geq 0.5$, the intersection of two modulating signals with the carrier results in a five-level output. The approach is to decompose the output waveform into two components and derive the Fourier coefficient for each of them. Then using the linearity property of Fourier series, the total harmonics can be obtained by summing the harmonics of each of the decomposed components. In this work, only linear modulation, i.e. $0 \leq m_i \leq 1.0$ is considered.

4.1 Derivation of Fourier Coefficient for Case of $m_i \leq 0.5$

With assumption that all dc sources of the five-level cascaded inverter have an equal value, the peak of the fundamental frequency component can be expressed as:

$$V_1 = m_i(2V_D) \quad (5)$$

Figure 4 shows the relationship between the modulating signals, carrier signal and PWM output voltage ($V_o(k)$). For simplicity the amplitude of $V_o(k)$ and the peak value of $c(k)$ are defined as 1 p.u. Since $V_o(k)$ is an odd signal with m_f pulses per cycle, the

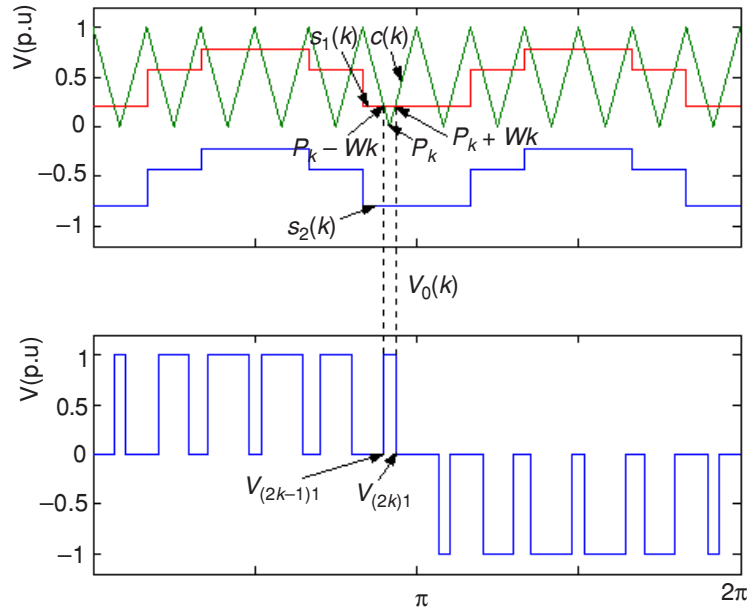


Figure 4 Relationship between the modulating signals, carrier signal and PWM output voltage $V_o(k)$ of a three-level inverter output

analysis can be reduced to first positive half cycle, resulting in the last k^{th} reduced to $\frac{m_f}{2}$. The discrete version of modulation signals for every k^{th} sample of $s_1(k)$ and $s_2(k)$ can be represented as:

$$s_1(k) = 2m_i \sin \left[\frac{(2\pi(k-1))}{m_f} + \frac{\pi}{m_f} \right]; \quad k = 1, 2, 3, \dots, \frac{m_f}{2} \quad (6)$$

$$s_2(k) = 2m_i \sin \left[\frac{(2\pi(k-1))}{m_f} + \frac{\pi}{m_f} \right] - 1; \quad k = 1, 2, 3, \dots, \frac{m_f}{2} \quad (7)$$

With the peak value of carrier signal equals 1 p.u, and by referring to Figure 5, $c(k)$ can be written as:

$$c(k) = \left| \frac{m_f \varpi}{\pi} + 1 - 2k \right| \quad \text{for} \quad \frac{(2k-2)\pi}{m_f} \leq \varpi \leq \frac{2k\pi}{m_f} \quad (8)$$

As shown in Equation (8), ϖ is valid between $\frac{(2k-2)\pi}{m_f}$ and $\frac{2k\pi}{m_f}$.

Derivation of Equation (8) could be understood by referring Figure 5

From Figure 5, for $\frac{(2k-2)\pi}{m_f} \leq \varpi \leq \frac{2k\pi}{m_f}$ carrier signal, $c(k)$ can be expressed as:

$$c(k) = |m| \varpi + d$$

Where $|m|$ is the slope and d is interception at $c^-(k)$ axial when $\varpi = 0$.

From the figure, value of m can be found from:

$$|m| = \left| \frac{1-0}{\frac{2k\pi}{m_f} - \frac{(2k-1)\pi}{m_f}} \right| = \left| \frac{m_f}{\pi} \right|$$

Therefore, positive slope carrier signal, $c^+(k)$ can be expressed as:

$$c^+(k) = \frac{m_f}{\pi} \varpi + d$$

Solving for d , when $\varpi = \frac{2k\pi}{m_f}$ yields $d = 1 - 2k$. Hence,

$$c^+(k) = \frac{m_f \varpi}{\pi} + 1 - 2k, \quad k = 1, 2, 3, \dots, \frac{m_f}{2} \quad (9)$$

Using similar method, negative slope of carrier signal, $c^-(k)$ can be expressed by:

$$c^-(k) = \left(-\frac{m_f}{\pi} \right) \varpi + (2k - 1), \quad k = 1, 2, 3, \dots, \frac{m_f}{2} \quad (10)$$

The k^{th} transition point as can be seen in Figure 5 is denoted by P_k , where:

$$P_k = \frac{(2k-1)}{m_f}; \quad k = 1, 2, 3, \dots, \frac{m_f}{2} \quad (11)$$

Let $\alpha_{(2k-1)1}$ and $\alpha_{(2k)1}$ represents the intersection of the carrier signal and sampled $s_1(k)$ within the k^{th} notch, such that:

At the point of intersections, $s_1(k) = c^-(k)$ for $\alpha_{(2k-1)1}$, it can be written that:

$$s_1(k)|_k = c^-(k)|_{\alpha_{(2k-1)1}}$$

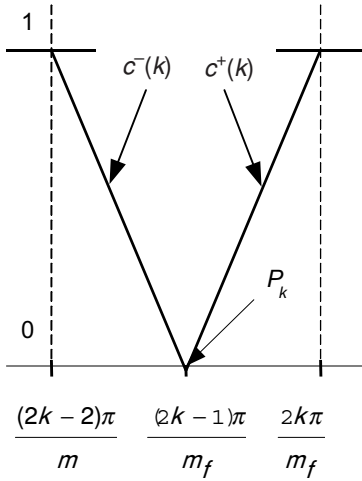


Figure 5 Carrier signal equation illustration

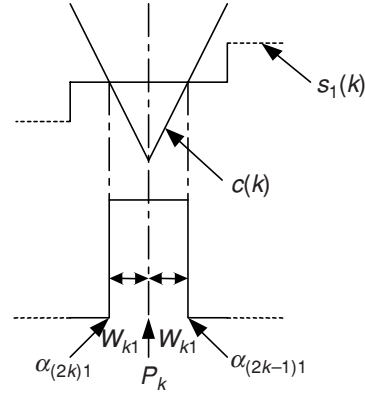


Figure 6 Half width (W_{k1}) of the PWM output waveform

$$\Rightarrow 2m_i \sin \left[\frac{2\pi(k-1)}{m_f} + \frac{\pi}{m_f} \right] = \left(-\frac{m_f}{\pi} \right) (\alpha_{(2k-1)1}) + 2k - 1$$

Since the m_i of five-level inverter is expressed by:

$$m_i = \frac{A_m}{2A_c}$$

Then the above equation can be rewritten as:

$$\alpha_{(2k-1)1} = P_k - \frac{2\pi m_i}{m_f} \sin(P_k) \tag{12}$$

and for $\alpha_{(2k)1}$

$$\alpha_{(2k)1} = P_k + \frac{2\pi m_i}{m_f} \sin(P_k) \tag{13}$$

To aid mathematical formulation, the half width (W_{k1}) of the output waveform in k^{th} pulse as shown in Figure 6 can be written as:

$$W_{k1} = \frac{\alpha_{(2k)1} - \alpha_{(2k-1)1}}{2} = \frac{2\pi m_i}{m_f} \sin(P_k) \tag{14}$$

Then the intersections within the k_{th} notch is expressed by:

$$\alpha_{(2k-1)1} = P_k - W_{k1} \quad (15)$$

$$\alpha_{(2k)1} = P_k + W_{k1} \quad (16)$$

The $V_o(k)$ transfer function is represented by:

$$V_o(k) = \begin{cases} +1 & \text{for } \alpha_{(2k-1)1} \leq \alpha_{(2k)1} \quad \text{and} \quad 1 \leq k \leq \frac{m_f}{2} \\ -1 & \text{for } \alpha_{(2k-1)1} \leq \alpha_{(2k)1} \quad \text{and} \quad \frac{m_f}{2} \leq k \leq m_f \\ 0 & \text{otherwise} \end{cases} \quad (17)$$

Using Fourier series, $V_{out}(k)$ can be expressed by:

$$V_o(k) = \frac{a_0}{2} + \sum_{n=-\infty}^{\infty} a_n \cos(n\omega_0 t) + b_n \sin(n\omega_0 t) \quad (18)$$

Since $V_o(k)$ is an odd function with m_f pulses per cycle and taking advantage of the symmetry, i.e. $a_0 = a_n = 0$, the above equation can be expressed as:

$$V_o(k) = \sum_{n=-\infty}^{\infty} b_n \sin(n\omega_0 t) \quad (19)$$

and

$$b_n = \frac{2}{\pi} + \int_0^{\pi} V_o(t) \sin(n\omega_0 t) d\omega_0 t \quad (20)$$

Evaluating the integration in Equation (20) by substituting the expression for and yields:

$$b_n = \frac{2}{\pi} + \sum_1^{\frac{m_f}{2}} \{ \cos[n(P_k + W_{k1})] - \cos[n(P_k - W_{k1})] \} \quad (21)$$

Using trigonometry identity, and normalizing Equation (21), can be reduced to:

$$\therefore b_n = \frac{2}{n\pi} + \sum_1^{\frac{m_f}{2}} [\sin(nP_k) \sin(nW_{k1})] \quad (22)$$

Substituting expression for P_k and W_{k1} from Equations (11) and (14) respectively, Equation (22) can be used to calculate the n^{th} harmonic for a five-level inverter when $m_i \leq 0.5$ using the proposed modulation scheme.

4.2 Derivation of Fourier Coefficient for Case of $0.5 < m_i \leq 1$

As previously mentioned, the proposed modulation scheme produces a five-level inverter output when $0.5 \leq m_i \leq 1$. Figures 7 and 8 show the decomposed output voltage i.e. $V_1(k)$ and $V_2(k)$, constructed from the intersection between the modulation signals and the carrier. Each dc power supply is assumed to be fixed at 1 p.u. Similarly, the amplitudes of $V_1(k)$ and $V_2(k)$ are defined as 1 p.u, respectively. By using the property of linearity in FFT, i.e.: $ax(t) + by(t) = ax(j\omega) + by(j\omega)$, the output harmonics of the five level output can be obtained. Figure 9 illustrates $V_1(k)$, i.e. the PWM waveform that is produced by the intersection between $c(k)$ and $s_1(k)$. $V_1(k)$ transfer function can be expressed by:

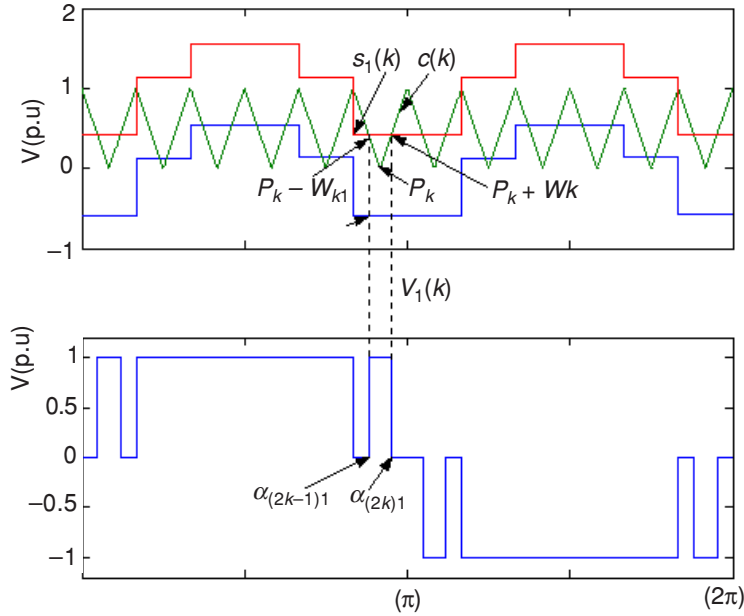


Figure 7 Intersection between $s_1(k)$ and $c(k)$ produces $V_1(k)$ pulses

$$V_i(k) = \left\{ \begin{array}{l} +1 \text{ for } \alpha_{(2k-1)1} \leq \alpha_{(2k)1} \text{ with } 1 \leq k \leq \bar{k} - 1 \text{ and } \frac{m_f}{2} - (\bar{k} - 2) \leq k \leq \frac{m_f}{2} \\ +1 \text{ for } \alpha_{(2k-1)1} \text{ until } \alpha_{\left(2\left(\frac{m_f}{2} - (\bar{k} - 1)\right) - 1\right)1} \\ -1 \text{ for } \alpha_{(2k-1)1} \leq \alpha_{(2k)1} \text{ and } \frac{m_f}{2} + 1 \leq k \leq \frac{m_f}{2} + \bar{k} - 1 \text{ and } m_f - (\bar{k} - 2) \leq k \leq m_f \\ -1 \text{ for } \alpha_{\left(2\left(\frac{m_f}{2} - (\bar{k} - 1)\right) - 1\right)1} \text{ until } \alpha_{(2(m_f - (\bar{k} - 1)) - 1)1} \\ 0 \text{ otherwise} \end{array} \right\} \quad (23)$$

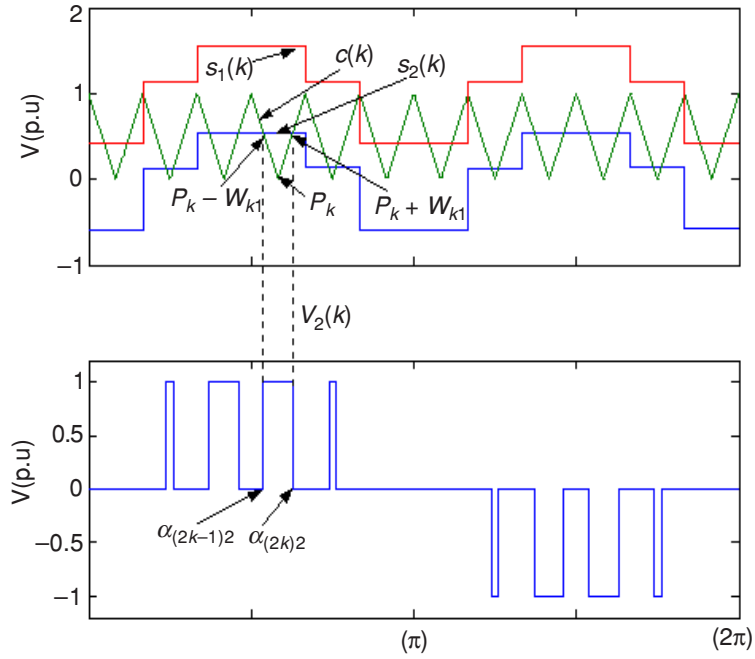


Figure 8 Intersection between $s_2(k)$ and $c(k)$ produces $V_2(k)$ pulses

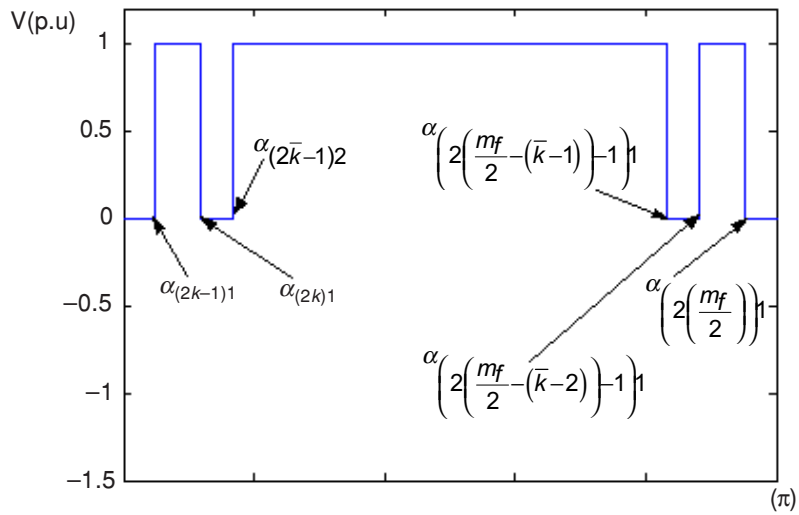


Figure 9 Range of $V_1(k)$ transfer function

Where \bar{k} is defined as the transition instant from $V_1(k)$ to $V_2(k)$ using natural sampling. The transition time of natural modulating signal from one level to another level can be expressed as:

$$t = \frac{\sin^{-1} \frac{1}{2m_i}}{2\pi f_o}$$

can be computed from t_o and m_f , which their relationship can be expressed as below;

$$\bar{k} = \left(\frac{t}{t_o} \right) m_f + 0.5 \quad \text{where; } t_o = \frac{1}{f_o} \quad (24)$$

However, \bar{k} in the above equation is not an integer; it must be rounded up to the nearest integer, as the value of k must always be an integer. Since k is an integer number started from 1, 2, 3 up to m_f , \bar{k} should be added with 0.5 to ensure its value is not started from 0.

Using the same procedure described in Section 4.1, i.e. substituting P_k from Equation (11) and W_{k1} from Equation (14) Fourier coefficient b_{n1} for $V_1(k)$ can be simplified expressed as:

$$b_{n1} = \frac{4}{n\pi} \sum_1^{\frac{m_f}{2}} [\sin(nP_k) \sin(nW_{k1})] - \frac{4}{n\pi} \sum_k^{\frac{m_f}{2} - (\bar{k}-2)} [\sin(nP_k) \sin(nW_{k1})] + \frac{2}{n\pi} \left\{ \cos(n\alpha_{(2\bar{k}-1)1}) - \cos \left(n\alpha_{(2(\frac{m_f}{2} - (\bar{k}-1)) - 1)1} \right) \right\} \quad (25)$$

For $V_2(k)$ analysis, the transfer function is determined by the intersection between $s_2(k)$ and $c(k)$. Let $\alpha_{(2k-1)2}$ and $\alpha_{(2k)2}$ represent the intersection between the carrier signal and sampled $s_2(k)$ within the k^{th} notch, where:

$$P_k - \left(\frac{\pi}{m_f} \right) \leq \alpha_{(2k-1)2} < \alpha_{(2k)2} \leq P_k + \left(\frac{\pi}{m_f} \right) \quad (26)$$

At the point of intersections between $s_2(k)$ and $c(k)$.

For $\alpha_{(2k-1)2}$

$$s^2(k) | k = c^-(k) | \alpha_{(2k-1)2}$$

Then,

$$A_m \sin \left[\frac{2\pi(k-1)}{m_f} + \frac{\pi}{m_f} \right] - 1 = A_c \left(\left(-\frac{m_f}{\pi} \right) (\alpha_{(2k-1)2}) + 2k - 1 \right)$$

Solving for $\alpha_{(2k-1)2}$,

$$\alpha_{(2k-1)2} = P_k + \frac{\pi}{m_f} - \frac{2\pi m_i}{m_f} \sin(P_k) \quad (27)$$

Similarly for $\alpha_{(2k)2}$

$$\alpha_{(2k)2} = P_k - \frac{\pi}{m_f} + \frac{2\pi m_i}{m_f} \sin(P_k) \quad (28)$$

By rearranging Equation (27) and (28), the half width (W_{k2}) of the output signal in k^{th} pulse can be define as:

$$W_{k2} = \frac{\alpha_{(2k)2} - \alpha_{(2k-1)2}}{2} = \frac{2\pi m_i}{m_f} \sin(P_k) - \frac{\pi}{m_f} \quad (29)$$

Wherein, the intersections between $s_2(k)$ and $c(k)$ within the k^{th} notch can be rewritten as:

$$\alpha_{(2k-1)2} = P_k - W_{k2} \quad (30)$$

$$\alpha_{(2k)2} = P_k + W_{k2} \quad (31)$$

Figure 10 shows the range of $V_2(k)$ transfer function for positive half cycle. $V_2(k)$ is constructed from the intersection between $c(k)$ and $s_2(k)$ as illustrated in Figure 8.

Its transfer function can be expressed as:

$$V_2(k) = \left\{ \begin{array}{l} +1 \quad \text{for} \quad \alpha_{(2k-1)1} \leq \alpha_{(2k)2} \quad \text{and} \quad \bar{k} \leq k \leq \frac{m_f}{2} - (\bar{k} - 1) \\ -1 \quad \text{for} \quad \alpha_{(2k-1)1} \leq \alpha_{(2k)2} \quad \text{and} \quad \frac{m_f}{2} + \bar{k} \leq k \leq m_f - (\bar{k} - 1) \\ 0 \quad \text{otherwise} \end{array} \right\} \quad (32)$$

Since $V_2(k)$ is also an odd signal, taking advantage of the symmetry, b_{n2} can be expressed as:

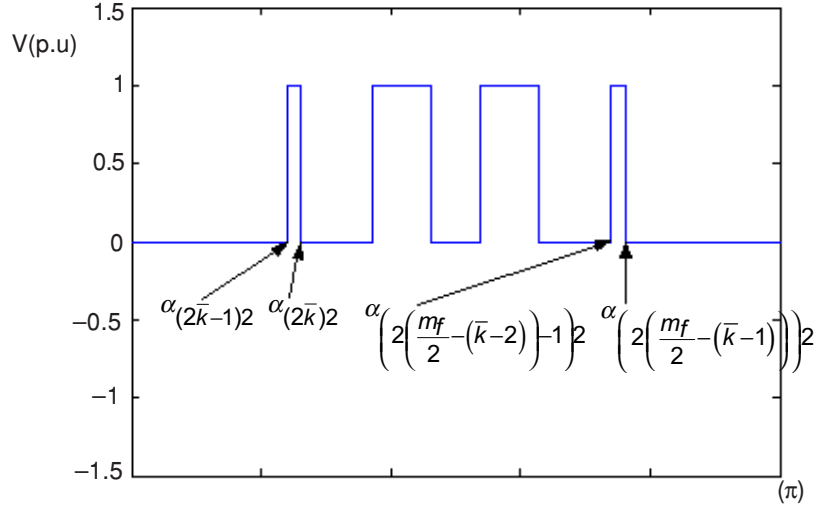


Figure 10 Range of $V_2(k)$ transfer function

$$\therefore b_{n2} = \frac{4}{n\pi} + \sum_k^{\frac{m_f}{2} - (\bar{k}-1)} [\sin(nP_k) \sin(nW_{k2})] \quad (33)$$

Since b_{n1} and b_{n2} are earlier defined as 1 p.u. Therefore the Fourier coefficient (b_n) for a five-level inverter output which is the sum of b_{n1} and b_{n2} can be written as:

$$b_2 = \frac{b_{n1} + b_{n2}}{2} \quad (34)$$

Hence the Fourier coefficient for a five-level output voltage using the proposed modulation scheme can be described as:

$$b_n = \frac{2}{n\pi} + \sum_1^{\frac{m_f}{2}} [\sin(nP_k) \sin(nW_{k1})] + \frac{2}{n\pi} + \sum_k^{\frac{m_f}{2} - (\bar{k}-1)} [\sin(nP_k) \sin(nW_{k2})] - \frac{2}{n\pi} + \sum_k^{\frac{m_f}{2} - (\bar{k}-1)} [\sin(nP_k) \sin(nW_{k1})] + \frac{1}{n\pi} \left\{ \cos(n\alpha_{(2\bar{k}-1)1}) - \cos\left(n\alpha_{(2(\frac{m_f}{2} - (\bar{k}-1)) - 1)1}\right) \right\} \quad (35)$$

4.3 Program Structure to Compute the Harmonics

From the derived harmonics equations, i.e Equations (22) and (35), the spectra of output voltage for a five-level inverter using the proposed modulation scheme can be calculated using MATLAB. The flow chart of the algorithm is illustrated in Figure 11. Recall that, the modulation must be in linear region i.e. $0 \leq m_i \leq 1.0$.

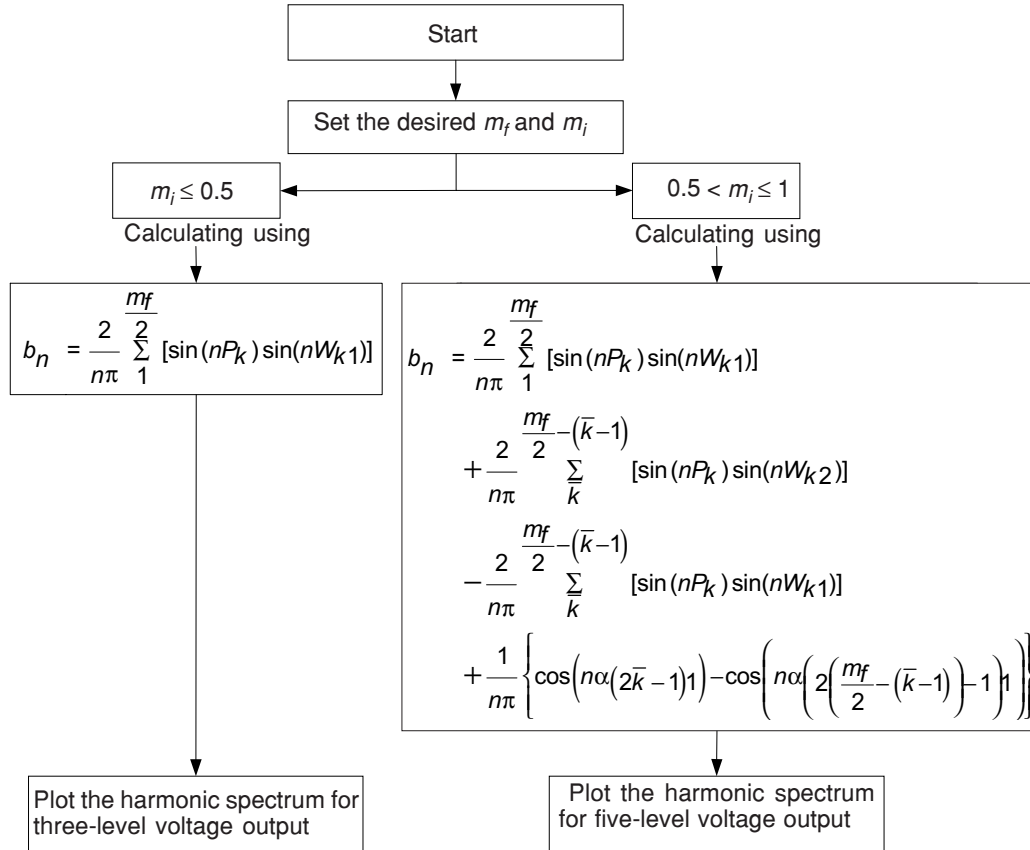
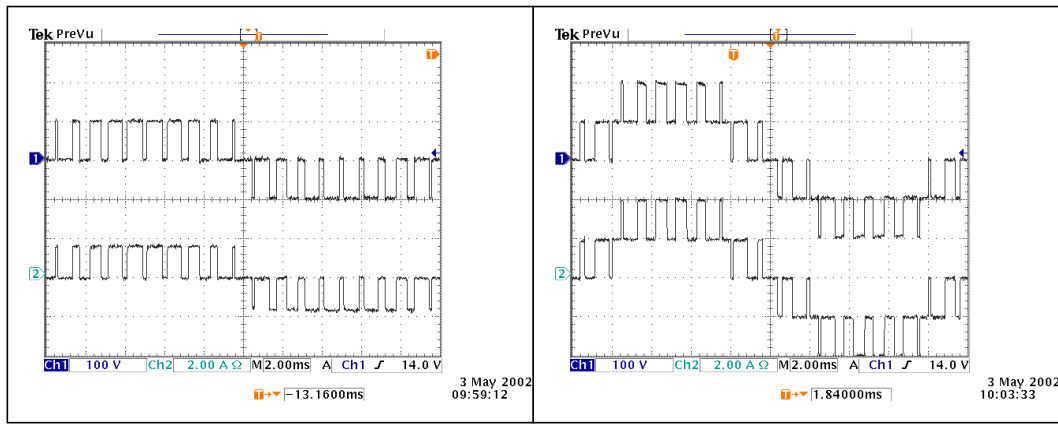


Figure 11 Flow chart for harmonic spectrum program

5.0 EXPERIMENTAL RESULTS

To validate harmonics equations derived previously; a five-level cascaded VSI is constructed. Equations (4.1) and (4.2) are used to generate the PWM signals for a single-phase five-level cascaded inverter. The generation is implemented using a relatively simple, 16-bit fixed-point microcontroller (SIEMENS SAB-C167CR-LM). The inverter input voltages are fixed at 100V dc for each module and the inverter load is a purely resistive.

Figures 12 (a) shows the oscillogram of the output voltage and current of the inverter for $m_i = 0.4$ and $m_f = 20$. Note that since $m_f \leq 0.5$, the output voltage is similar to the



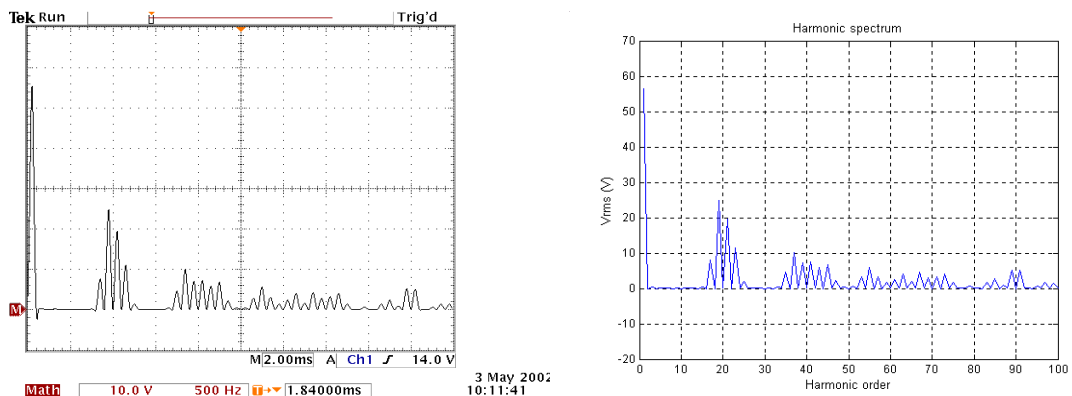
(a)

(b)

Figure 12 (a) Experimental result for $m_i = 0.4$; $m_f = 20$. (b) Experimental result for $m_i = 0.8$; $m_f = 20$. Top trace: Output voltage. Vertical scale 100V/div. Bottom trace: Output current. Vertical scale 2A/div. Horizontal scale 2ms/div

normal three level inverter. For the case of $m_i = 0.8$ and $m_f = 20$ shown in Figures 12 (b), the output has multilevel shape as described earlier.

The practical and theoretical output voltage harmonic spectrum are shown in Figures 13 (a) and (b), respectively. The latter is calculated using the derived equations for the case when $m_i \leq 0.5$, i.e. Equation (22). By comparing these two figures, it can be clearly observed that the harmonics incidences agree closely with theory. To demonstrate the accuracy between simulated and theoretical results, the value of the first harmonic cluster are tabulated in Table 1. It can be concluded that the results obtained from test-rig is in very good agreement with the theoretical predictions.



(a)

(b)

Figure 13 (a) Harmonic spectrum of output voltage for $m_i = 0.4$; $m_f = 20$. (b): Calculated values using Equation (22). Vertical scale 10V/div. Horizontal scale 500Hz/div

Table 1 Predicted and Measured Values of the First Harmonic Cluster for $m_i = 0.4$; $m_f = 20$.

Harmonic order	Frequency (Hz)	Magnitude of harmonic (V)	
		Predicted	Measured
17	850	8.0172	7.6
19	950	24.7733	24.8
21	1050	19.7115	19.8
23	1150	11.3250	11.4
25	1250	1.8777	1.6

Note: Predicted values are defined from the harmonic figures (after zoomed). Measured readings are taken directly from numerical values of harmonics given by Tektronix TDS3054 oscilloscope.

For the case of $m_f = 20$; $m_i = 0.8$, practical and theoretical results of the output voltage harmonic spectrum are illustrated in Figure 14 (a) and 14 (b), respectively. Again, it can be seen that as far as the harmonics incidences are concerned, the practical results agree with theory. Table 2 tabulates the predicted and numerical results of the first group of significant harmonics. In general, the simulation and practical results can be considered close enough to validate the correctness of the mathematical analysis.

To evaluate the modulation scheme performance at higher frequency, test at $m_i = 200$ is carried out. This ratio corresponds to inverter switching frequency of 10 kHz. The practical and simulation results for this case when modulation index equals 1.0 is shown in Figure 15 (a) and 15 (b), respectively. It can be seen that at high switching frequency, the practical result in a good agreement with the simulation result. The respective harmonic spectrum, as illustrated in Figure 16 (a) and 16 (b), are also consistent with each other.

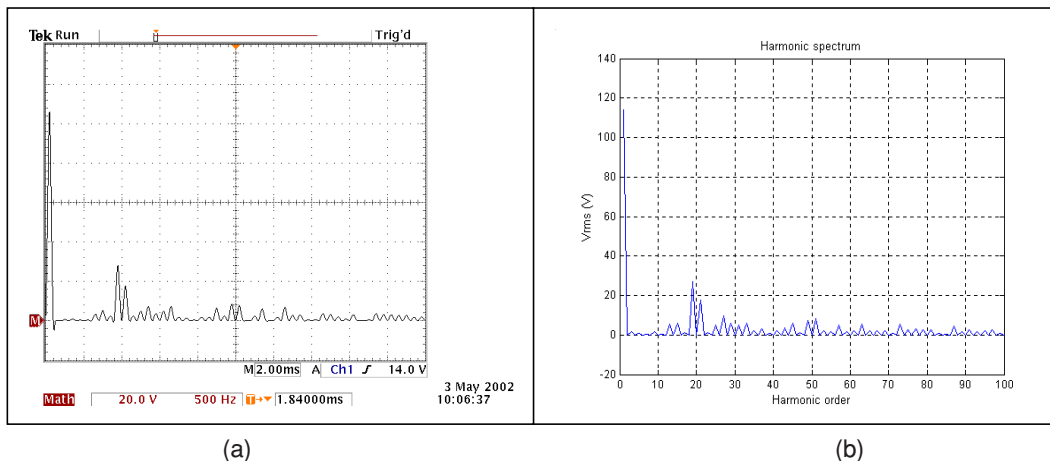
**Figure 14** (a) Practical harmonic spectrum of output voltage for $m_i = 0.8$; $m_f = 20$. (b) Calculated values using Equation (35). Vertical scale 20V/div. Horizontal scale 500Hz/div

Table 2 Predicted and Measured Values of the First Harmonic Cluster for $m_i = 0.8$; $m_f = 20$.

Harmonic order	Frequency (Hz)	Amplitude of harmonic (V)	
		Predicted	Measured
13	650	5.5870	5.4
15	750	5.9801	5.6
17	850	1.1052	1.2
19	950	26.9087	27.6
21	1050	17.4743	18.0

Note: Predicted values are defined from the harmonic figures (after zoomed). Measured readings are taken directly from numerical values of harmonics given by Tektronix TDS3054 oscilloscope.

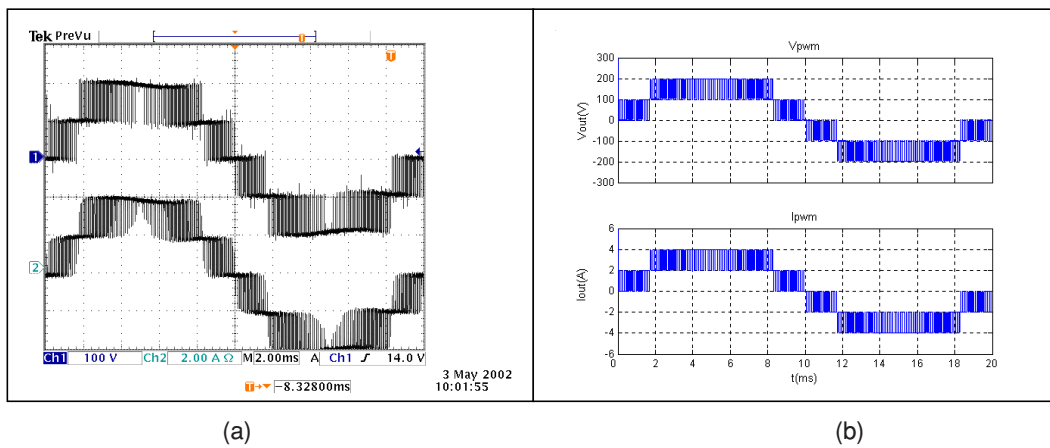


Figure 15 (a) Practical result for $m_i = 1.0$ $m_f = 200$. (b) Simulation. Top trace: Output voltage. Vertical scale 100V/div. Bottom trace: Output current. Vertical scale 2A/div. Horizontal scale 2ms/div

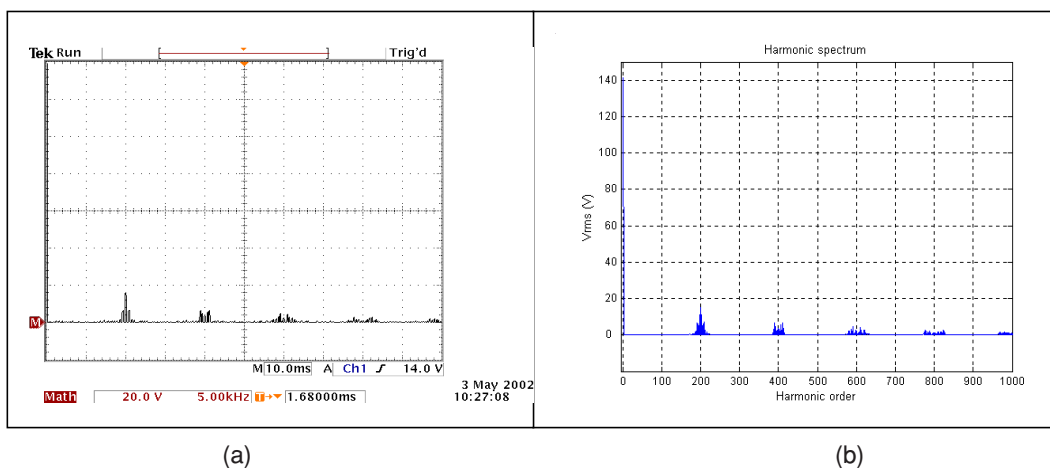


Figure 16 (a) Practical harmonic spectrum of output voltage for $m_i = 1.0$ and $m_f = 200$. (b) Calculated values using Equation (35). Vertical scale 20V/div. Horizontal scale 5kHz/div

It is worthwhile to note that the harmonic spectrum produced from the new modulation scheme is very similar with Phase Opposition Disposition (POD) scheme proposed by previous researchers [6]. This is because the end-results of both modulation techniques are quite similar although the approaches taken are significantly different. Traditional POD scheme uses a pure sinusoidal modulating signal modulated with several carrier signals, while the proposed scheme is using a single carrier signal modulated with several modified sinusoidal modulating signals.

5.1 Generalized of Harmonics Table for Five-level Inverter

The harmonics in the PWM inverter output voltage waveform appear as sidebands, clustered around the switching frequency and its multiples, i.e. m_f , $2m_f$, $3m_f$ etc. This general pattern is true for all values of m_i in the range 0 through 1.0. Table 3 attempts to generalize the harmonic amplitudes with respect to the fundamental voltage for a five-level inverter. The table is created using the calculated values from Equation (22) and (35).

The amplitude of sidebands harmonic in multilevel inverter output voltage waveform is somewhat larger when the inverter is switching at low frequency. The increase may be attributed to the overlaps that occur between the clusters when the modulation ratio is insufficiently high. From numerous trials, it was concluded that

Table 3 Generalized Harmonics of Voltage Output for Large m_f in Term of the Normalized Fundamental

m_i Fundamental	0.2 0.2	0.4 0.4	0.6 0.6	0.8 0.8	1.0 1.0
$m_f \pm 1$	0.1642	0.1632	0.1079	0.1542	0.0998
$m_f \pm 3$	0.0109	0.0656	0.0634	0.0145	0.0774
$m_f \pm 5$		0.0047	0.0624	0.0454	0.0010
$m_f \pm 7$			0.0076	0.0534	0.0425
$2m_f \pm 1$	0.0801	0.0523	0.0245	0.0049	0.0221
$2m_f \pm 3$	0.0339	0.0522	0.0425	0.0115	0.0185
$2m_f \pm 5$	0.0027	0.0445	0.0455	0.0375	0.0091
$2m_f \pm 7$			0.0442	0.0295	0.0358
$3m_f \pm 1$	0.0035	0.0163	0.0384	0.0155	0.0152
$3m_f \pm 3$	0.0442	0.0265	0.0182	0.0295	0.0035
$3m_f \pm 5$	0.0105	0.0338	0.0045	0.0145	0.0112
$3m_f \pm 7$		0.0286	0.0064	0.0179	0.0095
$4m_f \pm 1$	0.0262	0.0021	0.0161	0.0071	0.0075
$4m_f \pm 3$	0.0299	0.0055	0.0144	0.0085	0.0085
$4m_f \pm 5$	0.0204	0.0185	0.0088	0.0118	0.0022
$4m_f \pm 7$	0.0038	0.0157	0.0080	0.0138	0.0042

the minimum modulation ratio that guarantee no overlaps occurrence is 30. Therefore, the table is sufficiently accurate compared to experimental results for modulation ratio greater than 30. It can be observed that the amplitude of the fundamental component in the output voltage varies linearly with m_i . It also can be seen that the numbers of sidebands at the first significant harmonic group (m_f), increased in proportional to m_i .

5.2 Total Harmonic Distortion (THD)

Total Harmonic Distortion (THD) is the most common power quality index to describe the quality of power electronic converter [7,8]. In general, all the output voltage of power electronic converters is not purely sinusoidal. The THD of the output voltage can be defined as:

$$\text{THD} = \frac{\sqrt{\sum_{n=2}^{\infty} V_h^2}}{V_1} \quad (36)$$

Where n denotes the harmonic order and 1 is the fundamental quantity. For inverter application, THD represents how close the ac output waveform with pure sinusoidal waveform. A high-quality inverter system should have low THD.

Figure 17 shows the comparison of the THD between a five-level single-phase MSMI and a conventional two-level inverter configuration. The figure shows that for both cases, a poor THD are obtained when the inverter operated at low modulation index. This is to be expected because at $m_i \leq 0.5$, the MSMI essentially behaves like a conventional three-level inverter. A better THD is obtained when the inverter operated

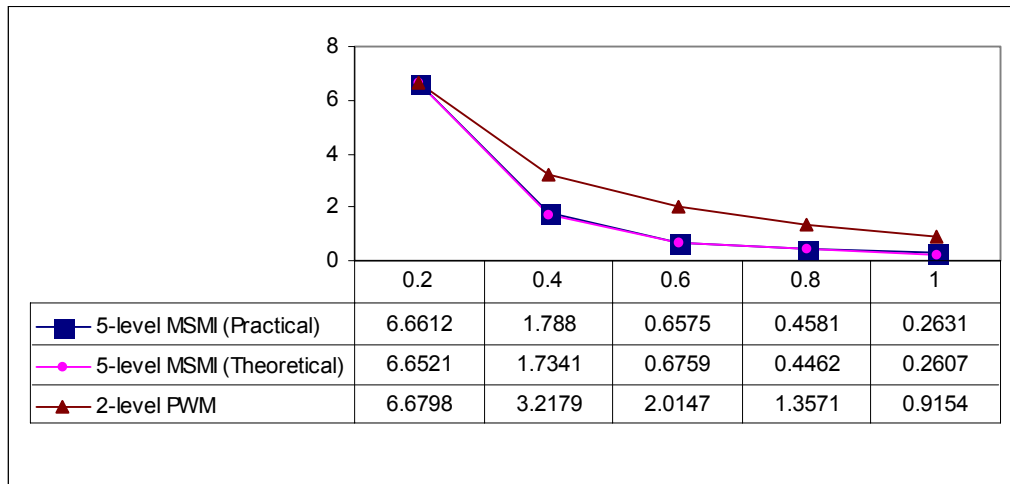


Figure 17 Variation of THD for five-level MSMI and two-level SPWM inverter configuration
Note: Data for two-level SPWM is obtained from Mohan et al [10].

at higher modulation index. For example, at modulation index equals 1.0, it was found that THD for a MSMI inverter is three times better compared to a conventional two-level inverter.

It is also worthwhile to note that for the MSMI, the calculated value of THD using the derived equations for the harmonics agree closely with the data obtained from the test-rig. It should be noted that for purpose of simplicity analysis was carried for one particular value of modulation ratio i.e. $m_f = 40$. However, it was found that for other values of m_f (above 30), the trend does not change very much. This is in conformity with the conclusion described in [9]. It is also important to note that the number of harmonics considered in all calculation above is only up to the fourth cluster.

6.0 CONCLUSIONS

This paper has described the method to calculate the harmonics of a five-level cascaded inverter using a new modulation scheme. Mathematical derivation of Fourier coefficient for a three-level (case of $m_i \leq 0.5$) and a five-level inverter (case of $0.5 m_i \leq 1$) waveform is outlined in detail. The resulting harmonic equations are programmed using MATLAB. The calculated spectra are compared with the spectra from the test rig. It can be concluded that the practical and theoretical results agreed closely for a wide range of modulation index and ratios. From the results, it was found that harmonic spectrum produced from the proposed modulation scheme is very similar to the POD technique described by other researchers.

ACKNOWLEDGEMENT

We wish to thank Malaysian Ministry of Science, Technology and Environment for the research sponsorship under Grant No. IRPA 72342.

REFERENCES

- [1] Ahmad Azli N., et al. 1998. Regular Sampled PWM Switching Strategies for A Modular Structured Multilevel VSI. *Journal of Technology 1998*. Universiti Teknologi Malaysia. 1-8.
- [2] Lai, J. S and F. Z Peng. 1995. Multilevel Converters – A New Breed of Power Converters. *Industry Applications Conf. 1995. Thirtieth IAS Annual Meeting, IAS '95. Conference Record of the 1995 IEEE*. 3: 2348-2356.
- [3] Li Li, et al. 2000. Multilevel Space Vector PWM Technique Based on Phase-Shift Harmonic Suppression. *Applied Power Electronics Conference and Exposition, 2000. APEC 2000. Fifteenth Annual IEEE*. 1: 535-541.
- [4] Zhang H., et al. 2000. Multilevel Inverter Modulation Schemes to eliminate Common-Mode Voltages. *IEEE Transactions on Industry Applications*. 36(6): 1645-1653.
- [5] Aziz, J. A. and Z. Salam. 2002. A PWM Strategy for Modular Structured Multilevel Inverter Suitable for Digital Implementation. *Accepted for IEEE International Power Electronics Congress. CIEP 2002, Guadalajara, Mexico October 20-24*.
- [6] Calais, M., L. J. Borle and V. G. Agelidis. 2001. Analysis of multicarrier PWM methods for a single-phase five level inverter. *Power Electronics Specialists Conference, 2001. PESC. 2001 IEEE 32nd Annual*. 3: 1351-1356.
- [7] Kandil, M. S., S. A. Farghal and A. Elmitwally. 2001. Refined Power Quality Indices. *Generation, Transmission and Distribution. IEE Proceedings*. 148(6): 590-596.

- [8] Abbas, M. H. 2000. Total Harmonic Distortion Analysis Simulation. International Conference on Power System Technology. 2000. *Proceedings*. PowerCon 2000. 3: 1631-1634.
- [9] Enjeti, P. N., P. D Ziogas, and J.F Lindsay, (1990). Programmed PWM Techniques to Eliminate Harmonics: A Critical Evaluation. *IEEE Transaction on Industry Applications*. 26(2): 302-316.
- [10] Mohan, N., T. M. Undeland and W. P. Robbins. 1995. *Power Electronics, Converters, Application and Design*. Second Edition. John Wiley & Sons, Inc. 207.

ABBREVIATIONS:

DC	= Direct Current
DCMI	= Diode-Clamped Multilevel Inverter
EMI	= Electromagnetic Interference
FCMI	= Flying-Capacitor Multilevel Inverter
MATLAB	= Matrix Laboratory
PWM	= Pulse Width Modulation